

# High-Yield Narrow-Band Matching Structures

DAVID H. MONTEITH AND JOHN E. PURVIANCE, MEMBER, IEEE

**Abstract**—Circuit yield is evaluated for commonly used narrow-band (bandwidth less than 5 percent) lumped and distributed parameter matching structures. It is found that yield is a function not only of the matching structure but also of the load impedance. The lumped structure yields are analytically determined using an elliptic approximation technique which gives a closed-form solution to the high-yield structure choice problem. Sensitivity issues are discussed. A simple design chart is developed which helps the designer choose a high-yield matching structure for a given load impedance. Two examples illustrate its use. Structure choice in one example changes the yield from 61 percent to 84 percent.

## I. INTRODUCTION

DURING THE manufacture of a mass-produced microwave amplifier, the amplifier parameters are subject to statistical variation due to uncertainties in the manufacturing process. Due to these parameter variations it is likely that some percentage of the total manufactured circuits will not meet the desired specifications. The fraction of circuits meeting the specification during manufacture is called the manufacturing yield, or simply yield.

There are three main ways to improve the manufacturing yield of a microwave amplifier. First the component tolerance can be decreased. However the tolerance is generally inversely proportional to the component cost, and components with a very narrow tolerance may not be available at any cost. In monolithic microwave integrated circuits (MMIC's), some parameters vary as much as  $\pm 17$  percent, with no easy way to reduce the variation [1]. The second way to improve the yield is through the process of design centering or statistical circuit design [2]. The drawbacks to this method of yield improvement are that the software is not readily available and it is very computer intensive for large circuits. The third method, the subject of this paper, is the use of the most tolerant structure for the design. Very little work has specifically dealt with this area [3]. Presently there are no published methods for choosing among narrow-band matching structure alternatives to find the one which gives the highest yield.

This paper presents the results of a study on the yield performance for some commonly used narrow-band microwave matching structures. The analytical methods developed here give a closed-form solution to the yield

Manuscript received April 19, 1988; revised August 2, 1988. This work was supported by Sandia National Laboratories, Albuquerque, NM, under Contract 02-5949.

The authors are with the Department of Electrical Engineering, University of Idaho, Moscow, ID 83843.

IEEE Log Number 8823776.

estimation problem for the simple lumped structures considered in this study. The results of this work give the design engineer a simple method for choosing among the matching structures studied to give the amplifier design with highest yield.

## II. ASSUMPTIONS

The purpose of this study is to evaluate and compare, using both analysis and simulation, the yield performance of some commonly used microwave narrow-band (bandwidth less than 5 percent) amplifier matching structures. The structures considered in this study are shown in Figs. 1 and 2. Fig. 1 shows the lumped parameter structures and Fig. 2 shows the distributed parameter structures. Each structure is given nominal parameter values which perfectly match the given load to the source.

To effectively limit the scope of this work, the following assumptions were made on the study:

- 1) Source impedance =  $50 \Omega$ .
- 2) 34 different load impedances were chosen. These values were chosen so they cover the entire Smith chart on lines of constant  $Q$  ( $Q = 0.5, 2$ , and  $5$ ). These are shown in Fig. 3.
- 3) The entire study was performed at one frequency, the center frequency of the designed match. The effects of frequency variation are not considered.
- 4) The source and load impedances were not varied. However simulation studies have indicated that the results shown here also apply to circuits where the load varies by as much as  $\pm 10$  percent.
- 5) A  $\pm 10$  percent variation was used on all circuit components.
- 6) The parameter statistics are uniform and uncorrelated.
- 7) The criterion applied to the circuit is  $|S_{11}|$  less than the specification. The specifications were chosen to allow yield comparison of circuits.

## III. YIELD CALCULATIONS

To determine the structures that possess the highest yield at a given load it is necessary to determine the yield at that load. The yield can be evaluated numerically, using Monte Carlo analysis for example, but the numerical evaluation does not give insight into the problem. In this section we develop an analytical method to determine the

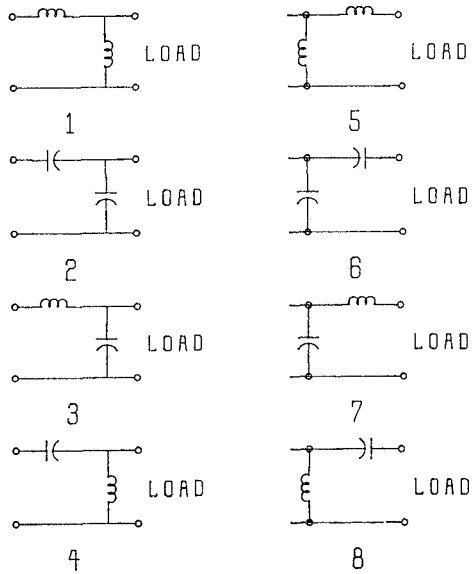


Fig. 1. Lumped parameter input–output matching structures.

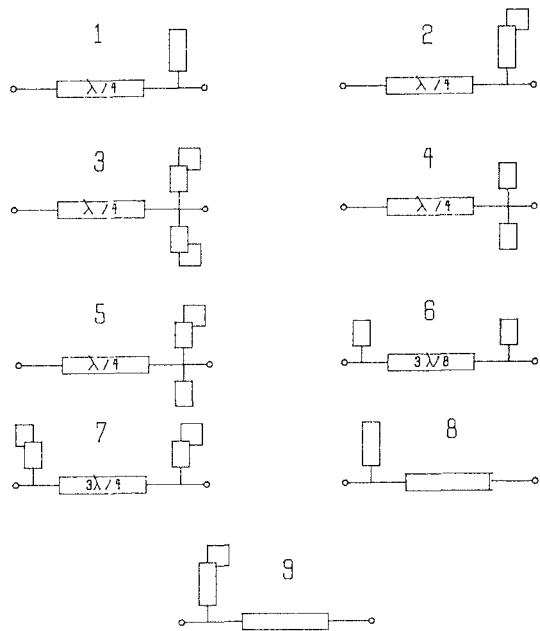


Fig. 2. Distributed parameter matching structures.

yield. This method is then applied to the narrow-band lumped element matching structures in Fig. 1. The analytical method provides insight into how component tolerances affect the yield and why there is yield symmetry in the final result. The method also determines in a closed form the lumped element structure that possesses the highest yield for a given load.

#### *A. Analytical Yield Estimation Approach*

1) *Definitions:* To understand the development of the method the following terms are defined. The parameter set is the set of all parameters necessary to define the circuit. The parameter space is the space of the parameter sets that define the circuit. Two subspaces of the parameter space are the acceptability region and the tolerance region. The acceptability region,  $R_A$ , is defined as the subspace which

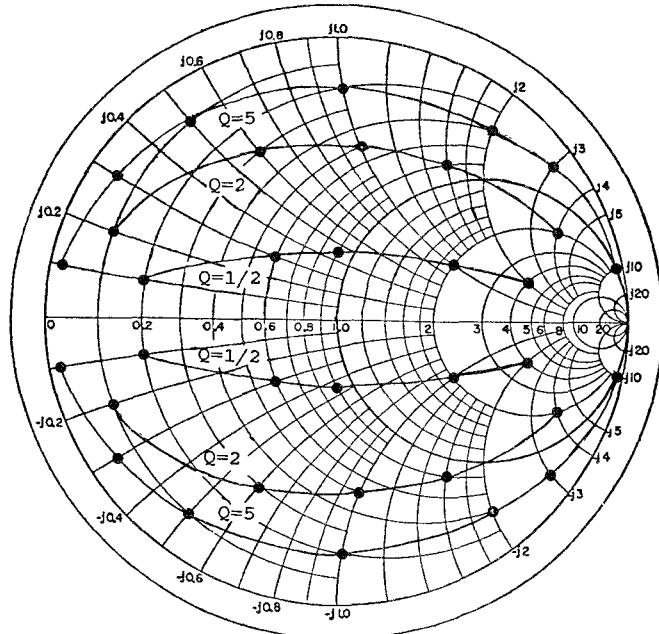


Fig. 3. The load impedances used in this study.

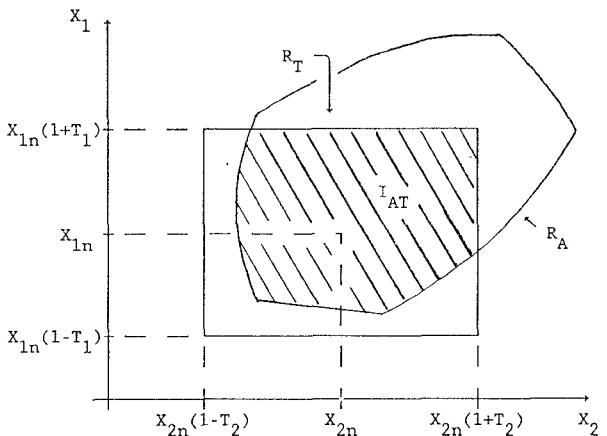


Fig. 4.  $R_T$ ,  $R_4$ , and  $I_{4T}$  represented in the two-dimensional parameter space given by  $X_1$  and  $X_2$ .

contains all possible parameter sets such that the circuit using these parameters meets specifications.  $R_A$  is defined by the design specifications applied to the circuit. The tolerance region,  $R_T$ , is the subspace that contains all possible parameter sets used during manufacture of the circuit.  $R_T$  is defined by the tolerance specifications associated with each parameter of the circuit. All circuits that meet the design specifications are represented by the members of  $R_A$ , and all circuits that can be encountered in manufacture are represented by the members of  $R_T$ . All circuits encountered in manufacture that meet specifications are represented by the members of the intersection of  $R_A$  and  $R_T$ , defined as the feasible region,  $L_T$  [4].

To better understand the above definitions, a two-dimensional example is given in Fig. 4. The nominal value for component one is  $X_{1n}$  and the tolerance value for component one is  $T_1$ . The respective values for component two are  $X_{2n}$  and  $T_2$ . In general, the acceptance region can be irregularly shaped, as shown. Using the assumptions of

uniform uncorrelated parameter statistics, the yield is the area of the intersection of  $R_A$  and  $R_T$  ( $I_{AT}$ ) divided by the area of  $R_T$ . This approach to yield calculation is used in the work that follows.

The irregularity of  $R_A$  is usually due to the different specifications that are applied to the circuit. For instance the shape of one side of the region may be due to a specification regarding the circuit gain and another side may be due to a specification regarding the input match. Because of the irregularity of  $R_A$  it is, in general, difficult to analytically compute  $I_{AT}$  directly. Thus it is equally difficult to compute the yield. It is for this reason that Monte Carlo techniques are a standard method used to calculate the area of  $I_{AT}$  and thus compute the yield of the circuit.

2) *The Elliptical Approximation Method:* We will develop in this section a closed-form solution for the yield estimate. This closed-form solution is useful for gaining insight into the circuit, as will be demonstrated in an example to follow. The problem with determining yield analytically lies in the shape of  $R_A$ . In general  $R_T$  is easily found using the parameter nominal and tolerance values, but  $R_A$  can be irregularly shaped and therefore its area is difficult to determine.

Director and Hachtel [5] have proposed a procedure for estimating  $R_A$ . This approach is based upon finding  $m > n$  points on  $R_A$  and connecting these points with straight lines to form a polyhedron, thus explicitly approximating the contour of  $R_A$  by a polyhedron made up of portions of  $n$ -dimensional hyperplanes which lie inside  $R_A$ . As  $m$ , the number of points on  $R_A$ , goes to infinity the polyhedron approaches  $R_A$ . A constraint applied to this procedure is that  $R_A$  and its complement be connected. The points on  $R_A$  are found by performing circuit simulations. One common method is to perform circuit simulations along an arbitrary vector in parameter space until the contour of  $R_A$  is found. This can be very computer intensive. In our method we analytically solve for the points on  $R_A$  in a closed form. This is done by determining an equation for the contour of  $R_A$  and finding the points along predetermined vectors.  $R_A$  is then approximated as a hyperellipsoid instead of a polyhedron. This usually gives a slightly better approximation of  $R_A$  when using a limited number of vectors because convex curves connect the points rather than straight lines. To make the calculation of the hyperellipsoid easier we choose the vectors which occur on the nominal parameter axes. The result of this approach is that the approximate  $R_A$ , defined as  $R'_A$ , is a smooth, connected region defined by a known algebraic equation. The expression for  $R'_A$  can be used to calculate a yield estimate and to gain further insight into the yield maximization problem.

An outline of the analytical yield estimation method is summarized below:

- Determine equations for the contour of  $R_A$ .
- Find the extent of  $R_A$  along the nominal parameter axes of the parameter space.

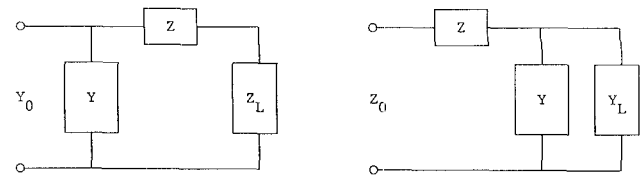


Fig. 5. The two general lumped parameter structures studied.

- Use the lengths of these axes in  $R_A$  to define a hyperellipsoid.
- Use the hyperellipsoid to approximate  $R_A$ .
- Approximate  $I_{AT}$  ( $I'_{AT}$ ) by computing  $R'_A \cap R_T$ .
- Calculate the yield estimate using  $I'_{AT}$  and  $R_T$ .

3) *Application:* As an example of how the analytical yield estimation method works it is now applied to the lumped element structures shown in Fig. 1. The method is used to determine the structures that give the highest yield for a given load. For these circuits  $R_A$  is connected and can be estimated. This fact can easily be seen later. From this estimate  $I_{AT}$  and its area are approximated.

For the lumped parameter matching structures in Fig. 1, there are two general structures of interest, shown in Fig. 5. The impedances  $Z$  and  $Y$  are both purely imaginary quantities; the loads,  $Y_L$  or  $Z_L$ , can have both real and imaginary parts; and  $Z_0$  is purely real. The constraints listed in the assumptions section are applied to these structures. Because only two of the circuit parameters are allowed to vary this is a two-dimensional problem.

To determine the contour of  $R_A$  we develop an expression for  $|S_{11}|$ .  $R_A$  is the region inside the contour found by setting  $|S_{11}|$  equal to the design specification on  $|S_{11}|$ . It should be noted that the two structures in Fig. 5 are duals of each other and therefore the resulting equations are duals. An example of this calculation for the second structure of Fig. 5 is presented below.

$$|S_{11}| = \frac{|-Z_0(Y + Y_L) + 1 + Z(Y + Y_L)|}{|Z_0(Y + Y_L) + 1 + Z(Y + Y_L)|}. \quad (1)$$

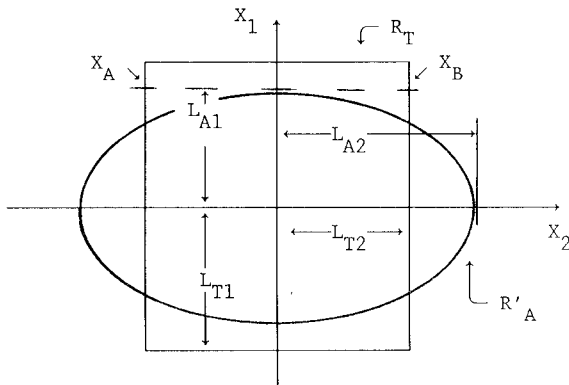
Now, using normalized variables, let

$$\begin{aligned} Z/Z_0 &= jx_1 \\ YZ_0 &= jb_2 \\ Y_L Z_0 &= g_L + y_L. \end{aligned}$$

Note that all load values can be represented and since  $Z$  and  $Y$  were originally stated to be purely imaginary, all of their values can also be represented. Note also that the contour of  $R_A$  is connected. Using the substitutions, (1) becomes

$$[1 - x_1(b_2 + b_L) - g_L]^2 + [x_1g_L - b_2 - b_L]^2 = \frac{4g_L|S_{11}|^2}{1 - |S_{11}|^2}. \quad (2)$$

The nominal values  $x_{1n}$  and  $b_{2n}$  are found by setting  $|S_{11}| = 0$ . This corresponds to the ideal match condition. The resulting equations for the nominal values are shown

Fig. 6. Example of a two-dimensional  $R'_A$  and  $R_T$ .

below:

$$x_{1n} = \pm \sqrt{\frac{1-g_L}{g_L}} \quad (3)$$

$$b_{2n} = \pm \sqrt{g_L(1-g_L)} - b_L. \quad (4)$$

determine the lengths of the nominal parameter axes:

$$\delta_{x1n} = L_{A1} = \frac{2|S_{11}|}{[1-|S_{11}|^2]^{1/2}} \quad (6)$$

$$\delta_{b2n} = L_{A2} = \frac{2g_L|S_{11}|}{[1-|S_{11}|^2]^{1/2}}. \quad (7)$$

An approximate  $I_{AT}$ ,  $I'_{AT}$ , can now be found by determining the relative widths of the axes of  $R'_A$  and the axes of  $R_T$ . Fig. 6 represents a sample  $R'_A$  and  $R_T$ . To explain how  $I'_{AT}$  is computed it is helpful to define  $L_{AM}$  and  $L_{TM}$ .  $L_{AM}$  and  $L_{TM}$  are the distance from the origin of the nominal parameter axis to the intersection of  $R'_A$  and  $R_T$  with the  $X_M$  axis, respectively. As can be seen in Fig. 6, there are two possible conditions: either  $L_{AM} > L_{TM}$  or  $L_{AM} < L_{TM}$ . The shorter of these lengths defines the extent of  $I_{AT}$  along the nominal axes.

The approximate yield can now be calculated by dividing the area of  $I'_{AT}$  by the area of  $R_T$ .  $R_T$  is rectangular and therefore its area is easily calculated:

$$\text{Yield} \approx W \frac{\min \left\{ \frac{\pm 2|S_{11}|g_L^{1/2}}{[(1-|S_{11}|^2)(1-g_L)]^{1/2}}, T_1 \right\} \min \left\{ \frac{2|S_{11}|g_L}{[(1-|S_{11}|^2)]^{1/2} \{ \pm [g_L(1-g_L)]^{1/2} - b_L \}}, T_2 \right\}}{4T_1 T_2} \quad (8)$$

Because of the complexity of  $R_A$  as given by (2), the area of  $R_A$  is difficult to compute; therefore  $R_A$  is approximated as an ellipse, as was outlined above. The lengths of the vectors along the nominal axes of  $R_A$  can be found by rewriting (2) in the form of a quadratic with respect to  $x_1$  with  $b_2 = b_{2n}$  and another quadratic with respect to  $b_2$  with  $x_1 = x_{1n}$ . The quadratic for  $x_1$  is as follows:

$$\delta_{x1} = \frac{1}{g_L^2 + (b_2 + b_L)^2} \cdot \left\{ \begin{array}{l} (b_2 + b_L)^2 \\ - [(b_2 + b_L)^2 + g_L^2][(g_L - 1)^2 + (b_2 + b_L)^2] \\ + \frac{4g_L|S_{11}|^2}{1-|S_{11}|^2} [(b_2 + b_L)^2 + g_L^2] \end{array} \right\}^{1/2} \quad (5)$$

$$\text{Yield} \approx W \frac{\min \left\{ \frac{\pm 2|S_{11}|r_L^{1/2}}{[(1-|S_{11}|^2)(1-r_L)]^{1/2}}, T_1 \right\} \min \left\{ \frac{2|S_{11}|r_L}{[(1-|S_{11}|^2)]^{1/2} \{ \pm [r_L(1-r_L)]^{1/2} - x_L \}}, T_2 \right\}}{4T_1 T_2}. \quad (9)$$

A similar quadratic for  $b_2$  is also determined. The nominal values are then substituted and the quadratic solved to

where

$$W = \begin{cases} \pi, & L_{AM} < L_{TM} \quad \text{for } M=1,2 \\ 4, & L_{AM} > L_{TM} \quad \text{for } M=1 \text{ or } M=2. \end{cases}$$

The reason for the weighting factor  $W$  can easily be seen in Fig. 6. When the weighting factor equals  $\pi$  then  $I'_{AT}$  equals  $R'_A$ , which is an ellipse. The area of an ellipse with radii  $a$  and  $b$  is  $\pi ab$ . For the other case the arcs which possibly form two sides of the  $I'_{AT}$  are very shallow and can be approximated as straight lines.

Equation (9) is the yield equation for the dual structure of Fig. 5(b), Fig. 5(a). The normalized variables of Fig. 5(a) are

$$YZ_0 = jb_1$$

$$Z/Z_0 = jx_2$$

$$Z_L/Z_0 = r_L + jx_L$$

Table I shows a comparison of the results obtained using the above approximations and the standard Monte

TABLE I  
COMPARISON OF THE ESTIMATED YIELD USING THE ANALYTICAL METHOD AND THE MONTE CARLO METHOD

STRUCTURE Fig. 1	$r_L + jx_L$	SPECIFICATION $ S_{11}  < -25\text{dB}$	ESTIMATED Analytical	YIELD Monte- Carlo	ERROR $ A_{\text{An}} - A_{\text{M.C.}} $ %
1	88-j 44	-40 dB	60.0%	58.6%	2.4%
1	25-j 0.5	-25 dB	74.7%	74.2%	0.7%
1	4-j 0.8	-25 dB	100%	90.1%	10%
1	67-j 1.3	-25 dB	73.7%	73.2%	0.7%
1	.06-j 32	-20 dB	48.1%	46.3%	3.8%
1	096-j 48	-20 dB	53.2%	51.3%	3.7%
1	38-j 1.9	-20 dB	67.0%	61.4%	9.1%
1	.64-j 3.2	-20 dB	50.8%	49.7%	1.8%
4	88-j .44	-30 dB	76.8%	73.0%	5.2%
4	1.3-j 67	-30 dB	28.5%	29.4%	3.0%
4	4-j 2	-30 dB	7.1%	7.9%	10%
4	4+j 2	-30 dB	10.8%	11.8%	8.5%
4	2+j 1	-30 dB	35.9%	37.1%	3.2%

Carlo method. As can be seen, the results using the approximation are quite close to the results using the Monte Carlo analysis. The largest errors, approximately 10 percent, occur when  $L_A$  is only slightly larger than  $L_T$  or when the estimated yield is small. The reason that the error is large for the first condition is that the straight-line approximation for the segment  $X_{AB}$ , as shown in Fig. 6, is poor. The reason error is large for the second case is the small size of  $R_A$ . In both cases the yield estimate could be improved by finding more points on  $R_A$ . Even though these errors do occur in some cases the results are still very useful for characterizing the yield behavior of the circuit at various loads and for giving a good first-order approximation of the yield with very little computational overhead.

4) *Structure Determination:* The structure with highest yield is found by putting the load values into (8) and (9) and comparing the yield estimates. The results of this procedure agree with the Monte Carlo analysis presented below. This procedure has an added benefit over the Monte Carlo analysis in that once the equations have been derived they can easily be programmed to give the result for any load impedance after only a few calculations, as opposed to the 1000 to 2000 circuit simulations required of a Monte Carlo analysis. The problem with this procedure is that when the mathematical description of the circuit becomes complicated, as in large or distributed element circuits, the equations required appear to be intractable.

5) *Results:* Fig. 7 presents the results of this work for the lumped parameter matching structures. Despite the large number of structures and load impedances considered in this study the results are very concise and are easily presented graphically on a Smith chart. Each arrow in Fig. 7 associates the highest yield structure for each region of load impedances on the Smith chart. The upper and the lower center of the Fig. 7 chart are covered by two structures. Both give good yield for most loads in this region. The one which gives the best yield can be determined from (8) and (9) or Monte Carlo simulations. This chart should be valuable to the designer since it gives a high-yield narrow-band matching structure for any load impedance.

### B. Sensitivity of Yield to Tolerance Variations

A useful by-product of calculating the yield approximation is that the sensitivity of the yield to the tolerance on each component is also determined. The sensitivity is based on the calculated widths of the  $R'_A$  and  $R_T$  main axes. This can best be seen by using Fig. 6 as an example. In this figure  $L_{A2} > L_{T2}$ . Since all circuits defined by points along  $X_2$  encountered in manufacturing are contained in  $R'_A$ , it is expected that the yield is insensitive to the tolerance changes on this component. The tolerance region along this axis could be increased with a minimal effect on the yield of the circuit. This could decrease the cost of the circuit. On the other hand, along the  $X_1$  axis  $L_{A1} < L_{T1}$ . Some of the circuits defined by points along  $X_1$  encountered in manufacturing will not meet the design specifications. Therefore, the yield is expected to be sensitive to the tolerance changes on this component. To improve the yield to an acceptable level it may be necessary to decrease the size of the tolerance region along this axis. These results can be summarized in the following two statements:

- If  $L_{Am} > L_{Tm}$  then the yield is relatively insensitive to changes in the tolerance of component  $m$ .
- If  $L_{Am} < L_{Tm}$  then the yield is sensitive to changes in the tolerance of component  $m$ .

### C. Symmetry

An interesting and useful result that is suggested in Fig. 7 is that the predicted yield for not only dual circuits but also conjugate circuits is the same. Conjugate circuits have the properties that:

- the conjugate circuits match complex conjugate loads;
- the structure of both circuits is the same;
- the impedance of each component is the complex conjugate of the corresponding component in the conjugate circuit.

An example of these characteristics is shown in Fig. 8.

At a single frequency the  $R_A$  for conjugate circuits is the same. This is easily proven using T-matrix circuit descriptions. If the tolerances on components are small (less than  $\pm 20$  percent) then  $R_T$  is approximately the same for conjugate circuits. These relationships hold for arbitrarily large circuits.

### D. Monte Carlo Simulation

In order to validate the results of the analytical analysis and to consider the mathematically more complicated distributed parameter structures, a standard Monte Carlo analysis was used for yield estimation. Monte Carlo analysis was chosen because of its accuracy and known convergence properties. Using the constraints on the parameters and loads listed above, each matching structure in Figs. 1 and 2 was analyzed with each load in Fig. 3 to determine the circuit yield. Table II shows typical yield calculations for the lumped parameter structures at different load impedances. These data are typical of those generated in

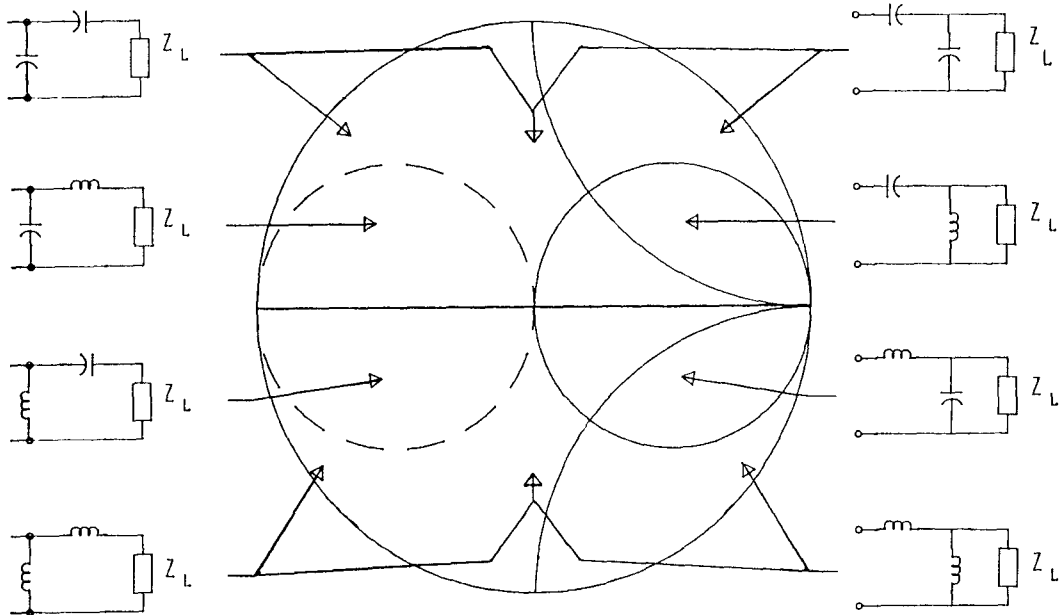


Fig. 7. Tolerant lumped parameter structures.

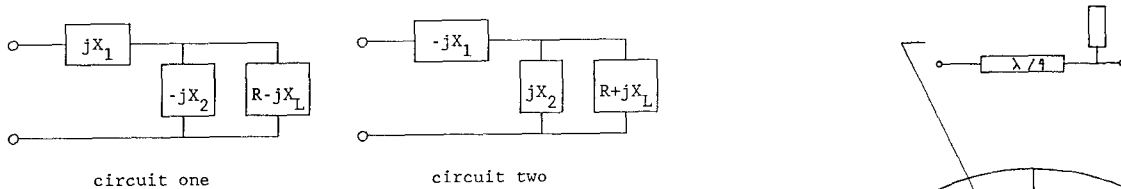


Fig. 8. An example of conjugate circuits.

TABLE II  
EXAMPLE MONTE CARLO YIELD CALCULATIONS FOR LUMPED  
PARAMETER MATCHING STRUCTURES

STRUCTURE (Fig 1)	LOAD IMPEDANCE (Normalized to 50Ω)					
	2-j4	.67-j1.3	1-j 2	1+j.2	67+j1.3	2+j4
1	--	73	--	--	--	--
2	--	--	--	--	72	--
3	36	--	--	--	21	11
4	11	22	--	--	--	35
5	--	83	--	--	--	--
6	--	--	--	--	84	--
7	--	41	11	36	--	--
8	--	--	36	10	42	--

The design specification is  $|S_{11}| < -25$  dB.

this study and are only a small fraction of the total data. In all, approximately 180 CPU hours on an HP 200 series computer were used in this study.

*Simulation Results:* Despite the mass quantities of data generated, the results of this study are very concise and are easily presented graphically on a Smith chart. Fig. 7 presents the results for the lumped element structures. As stated before, the Monte Carlo and analytical methods determined the same tolerant matching structures. Fig. 9 presents the results for the distributed element structures. Each arrow in these figures associates the high-yield structure for each region of load impedances on the Smith chart. As can be seen from Fig. 9, of all the distributed

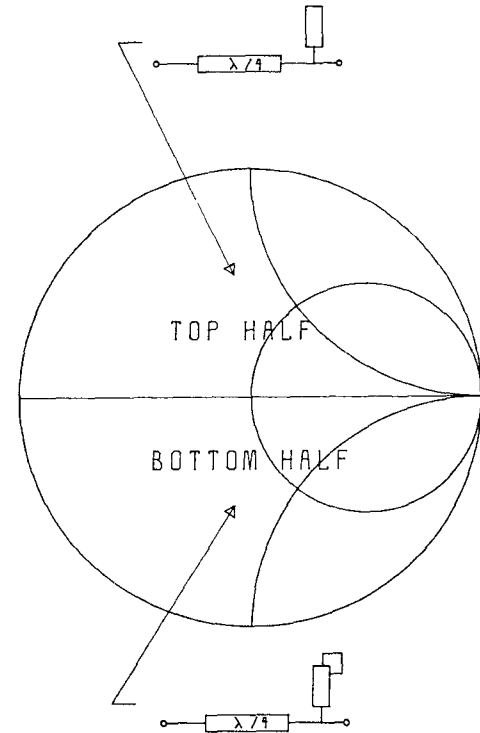


Fig. 9. Tolerant distributed parameter matching structures.

parameter structures only two consistently gave high yield for the load impedances studied. For load impedances in the top half of the Smith chart, the quarter-wave transformer and an open parallel stub consistently gave the highest yield; for load impedances in the bottom half of the Smith chart, a quarter-wave transformer and a shorted parallel stub gave the highest yield. At a few of the load impedances studied, the results of Fig. 9 were violated; however the high-yield structure had a yield only slightly higher than the given structure. Equations (8) and (9) and Figs. 7 and 9 give the design engineer a useful guideline for

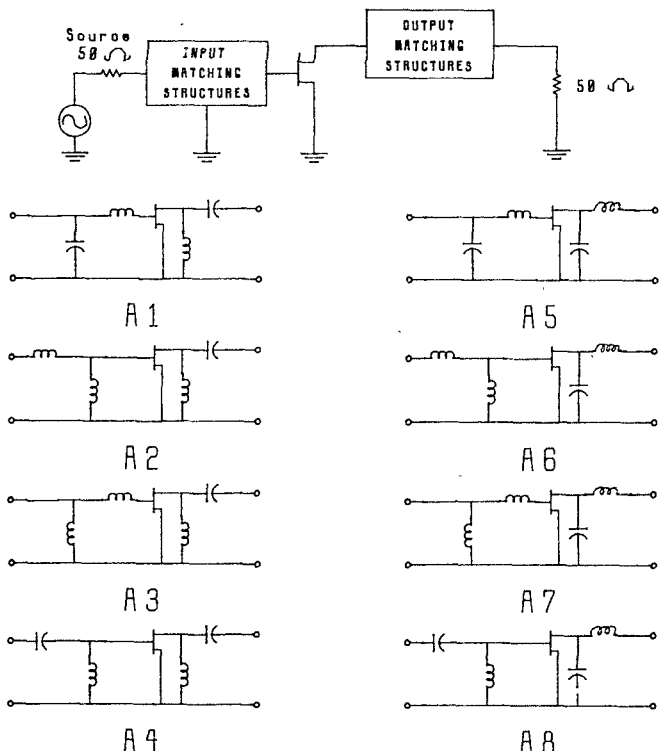


Fig. 10. Example 1 matching structures.

choosing the most tolerant matching structures for a narrow-band amplifier design. The effect of the structure choice on circuit yield can be significant, as is illustrated in the examples that follow.

#### IV. EXAMPLES

The following two examples illustrate the use of Figs. 7 and 9 to choose the most tolerant matching structure.

##### Example 1: Lumped Parameter Example

A 4 GHz single-stage amplifier design is examined. The specifications for the design are  $|S_{11}| < -20$  dB and  $|S_{22}| < -20$  dB, with no specification on  $S_{21}$ . This example uses lumped element matching structures to match the input and output to  $50 \Omega$ . The  $S$  parameters for the transistor at 4 GHz are

$$S_{11} = 0.52 \angle 80^\circ$$

$$S_{12} = 0$$

$$S_{21} = 2.0 \angle 80^\circ$$

$$S_{22} = 0.54 \angle -46^\circ.$$

The unilateral assumption was made on the transistor because the results of this study were developed using one-ports. All possible circuit configurations using the matching structures in Fig. 7 are shown in Fig. 10.

Plotting  $S_{11}$  and  $S_{22}$  on Fig. 7 shows that the high-yield input structure is series  $L$ , shunt  $L$  and that the high-yield output structure is shunt  $C$ , series  $L$ . Table III gives the yield calculation for each circuit shown in Fig. 10. As the table shows, structure A6 has the highest yield, as predicted by the Smith chart in Fig. 7. An important point to note from this example, aside from the fact that the Fig. 7

TABLE III  
EXAMPLE 1 YIELD CALCULATIONS

Design Numbers	Yield (Percent)
A1	68.2
A2	74.8
A3	66.9
A4	61.2
A5	78.9
A6	84.7
A7	76.0
A8	70.0

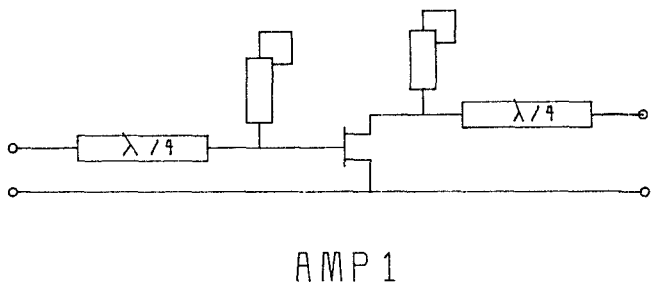


Fig. 11. Distributed parameter amplifier example.

Smith chart predicted the highest yield structure, is that the structure choice caused yield variations from 61.2 percent to 84.7 percent. The effect that structure has on circuit yield is not universally known, and as a result lower yield circuits are sometimes designed and manufactured.

##### Example 2: Distributed Parameter Amplifier Example

In this example, two amplifiers were designed to test the validity of the results of the distributed parameter Monte Carlo study. The  $S$  parameters (at 4 GHz) to be used are  $S_{11} = 0.895 \angle -33.53^\circ$ ,  $S_{12} = 0$ ,  $S_{21} = 2.5 \angle 95^\circ$ , and  $S_{22} = 0.821 \angle -91.27^\circ$ .

The first amplifier (amp 1) will use a quarter-wave line and a shorted stub matching structure for the input and the output. This amplifier is labeled #1 in Fig. 11. The second amplifier (amp 2) will use quarter-wave lines and open stubs and is labeled #2 in Fig. 11.

For this transistor both  $S_{11}$  and  $S_{22}$  are in the lower half of the Smith chart. From an examination of Fig. 9, amp 1 is predicted to have the highest yield. The two amplifiers were designed and a yield calculation was done for the specification:  $|S_{11}|$  and  $|S_{22}|$  both  $< -8$  dB, and no criteria on  $S_{21}$ . A  $\pm 10$  percent uniform distribution was used on

the line length and width parameters. The analysis was done at a single frequency. Amp 1 was found to have a yield of 23 percent and amp 2 was found to have a yield of 7 percent. Not only did amp 1 have the higher yield, as predicted, but its yield was three times higher! This dramatically demonstrates the effect that structure can have on manufacturing yield.

## V. CONCLUSIONS

One of the accomplishments of this paper is to demonstrate conclusively the strong effect that structure choice has on circuit yield. In the first example the circuit yield estimate improved from 61 percent to 84 percent when the circuit structure was changed. The main result of this paper is a design chart, in the form of Figs. 7 and 9, with which the design engineer can choose tolerant high-yield narrow-band matching structures. The analytical work develops a method for determining, in closed form, the lumped parameter matching structure with highest yield. The distributed parameter case proved too complex to be handled analytically. Both cases were studied using Monte Carlo simulations. The analytical work also determined the sensitivity of the yield estimate to parameter tolerances and proved a symmetry of yield estimates.

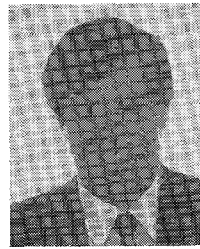
## ACKNOWLEDGMENT

The authors thank W. Brakensiek for helping with the extensive simulations used in this study and T. Ferguson for her insight into the initial aspects of this work. They would also like to thank the reviewers for some very helpful comments.

## REFERENCES

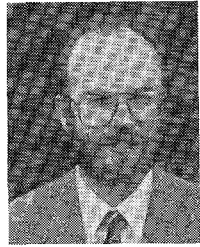
- [1] J. E. Purviance, D. Criss, and D. H. Monteith, "FET model statistics and their effects on design centering and yield prediction for microwave amplifiers," in *Proc. 1988 MTT-S Int. Conf.*, May 1988, pp. 315-318.
- [2] R. K. Brayton and R. Spence, *Sensitivity and Optimization*, vol. 2. Amsterdam, The Netherlands: Elsevier, 1980, ch. 12.
- [3] M. Kumar, G. Taylor, and H. Huang, "Design considerations for monolithic GaAs FET amplifier," presented at the 1980 GaAs Symposium.
- [4] R. S. Soin and R. Spence, "Statistical exploration approach to design centering," *Proc. Inst. Elec. Eng.*, vol. 127, no. 6, pp. 260-269, 1980.
- [5] S. W. Director and G. D. Hachtel, "The simplicial approximation approach to design centering," *IEEE Trans. Circuits Syst.*, vol. CAS-24, pp. 363-372, 1977.
- [6] A. MacFarland, *et al.*, "Centering and tolerancing the components of microwave amplifiers," in *Proc. 1987 MTT-S Int. Conf.*, June 1987, pp. 633-636.

★



**David H. Monteith** was born in Spokane, WA, on May 12, 1964. He received the B.S. and M.S. degrees in electrical engineering from the University of Idaho, Moscow, in 1984 and 1987, respectively. During his graduate studies, he held research and instructional assistantships in the microwave area. The subject of his master's thesis was the effect of matching structure changes on the yield of microwave amplifiers.

★



**John E. Purviance** (S'71-M'80) was born in Clarkston, WA, in 1948. He received the B.S.E.E. degree from the University of Idaho in 1972, the M.S.E.E. degree from Northwestern University in 1973, the Engr.E.E. degree from the University of Southern California in 1977, and the Ph.D. degree from the University of Idaho in 1980.

From 1973 to 1977 he was with the Space Communications Group of Hughes Aircraft Company. Since 1980 he has been an Assistant and an Associate Professor at the University of Idaho. His research activities include microwave circuit design and measurements, CAD for yield improvement, DSP, and systems theory.

Dr. Purviance is a member of the Instrument Society of America. He was a recipient of an IEEE outstanding advisor award in 1984, an outstanding faculty award in 1986, and several teaching awards. He was a NSF Fellow in 1973 and a Hughes Aircraft Fellow in 1974-1977.